Proceedings of the 21st ICSMGE, Vienna, Austria, 14 – 19 June 2026. Pistrol, Adam & Schweiger (eds.)
Published by: ÖGG, Austrian Society for Geomechanics, Salzburg, Austria, ISBN 978-3-9503898-4-5
https://doi.org/10.53243/ICSMGE2026-882

Analytical framework for stress-induced anisotropy in infinite sandy slopes under cyclic loading conditions

Revathy Manohar, Sireesh Saride
Dept. of Civil Engineering, Indian Institute of Technology Hyderabad, Telangana, India, sireesh@ce.iith.ac.in

ABSTRACT: Understanding the influence of stress-induced anisotropy under cyclic loading is essential for evaluating the stability of infinite sandy slopes subjected to seismic excitations. This study proposes a novel analytical framework that incorporates the effects of stress-induced anisotropy into the factor of safety (F_d) formulation for cohesionless slopes under earthquake-induced loading. The model considers key parameters such as slope angle (β), earth pressure coefficient (k_0), and seismic coefficients (k_h, k_v) to derive a dimensionless anisotropic stress ratio (k_c), which quantifies the directional stress response. The analysis aimed to study the effect of slope angle and stress-induced anisotropy on the stability of slopes under cyclic loading conditions. To compare and complement the analytical predictions, a series of experiments were conducted using an electro-mechanical dynamic cyclic simple shear (EMDCSS) device on sand under different k_0 conditions. Three slope configurations (β = 20^0, 30^0 and 45^0) were simulated by applying corresponding vertical stresses (σ_v = 26, 22.07, and 14.72 kPa). Cyclic loading was applied at 1 Hz frequency and 0.1 mm amplitude for 100 cycles. The cyclic stress ratio (CSR) was examined alongside hysteresis response and stiffness degradation across varying slope configurations. A regression analysis was performed between analytical predictions and experimental outcomes, confirming the consistency and reliability of the proposed model in capturing anisotropic soil behaviour under cyclic conditions. The relationship between CSR and the number of cycles (N) was studied to evaluate the model's performance under prolonged dynamic loading. This integrated approach demonstrates the practical applicability of incorporating anisotropy into seismic slope stability analysis, and the study offers a foundational basis for extending design methodologies in geotechnical earthquake engineering.

KEYWORDS: Stress-induced, anisotropy, slopes, cyclic loading.

1 INTRODUCTION

The mechanical behaviour of granular materials like sand is significantly influenced by anisotropy, which can be classified as inherent (originating from depositional processes) or stress-induced (arising due to applied loading). Under cyclic loading conditions, especially those mimicking earthquake-like events, the internal structure or fabric of sand evolves, leading to variations in its stiffness, strength, and deformation characteristics.

In infinite sandy slopes, stress-induced anisotropy plays a crucial role in determining stability, particularly under undrained and repeated loading scenarios. This phenomenon arises due to changes in the orientation of principal stresses and strain paths, which continuously modify the granular contact network and pore pressure response. Understanding this anisotropic response is key to predicting failure mechanisms such as cyclic mobility and liquefaction, which are often triggered in gently sloping sandy deposits during seismic events (Manohar and Saride, 2025).

Numerous studies (Shi et al., 2010; Gao, 2013) have highlighted the limitations of isotropic models in capturing the true cyclic response of sands. Anisotropic models, incorporating fabric tensors and directional strength variations, have shown better accuracy in simulating cyclic strain accumulation and pore pressure generation. (Fakharian, Kaviani-Hamedani and Imam, 2022) and (Chen et al., 2020) emphasised that the undrained cyclic behaviour of sand is highly sensitive to both initial fabric and the imposed cyclic stress paths, especially under anisotropic conditions.

Despite advancements, existing models often face challenges in comprehensively addressing stress-induced anisotropy without relying on complex adjustments for different density states or loading paths. For instance, (Asaoka et al., 2002) introduced a model describing collapse in loose sands but could not capture cyclic mobility in medium-dense sands. (Zhang et al., 2007) improved upon this by proposing evolution rules based on stress-induced anisotropy and overconsolidation changes. While simplified models are essential for practical seismic slope analysis, they often overlook key soil behaviours. (Biondi et al., 2000) proposed a method based on the Newmark sliding block approach to evaluate seismic displacements in saturated sandy slopes, incorporating pore pressure build-up through empirical correlations. However, their model assumes a rigid slope response and neglects stress-induced anisotropy and fabric evolution during cyclic loading. This can lead to inaccurate predictions, especially for medium-dense sands under prolonged shaking.

In this context, this study presents a simplified analytical framework that explicitly accounts for stress-induced anisotropy in cohesionless infinite slopes under cyclic loading. The proposed model offers a mechanistic interpretation of anisotropic effects on slope stability and is compared with a set of cyclic simple shear experiments performed at varying slope inclinations. The comparison is expressed in terms of cyclic stress ratio (CSR) and provides insight into how slope angle and stress anisotropy together influence the cyclic resistance of sand.

2 ANALYTICAL MODELING

2.1 *Formulation of anisotropic stress ratio*

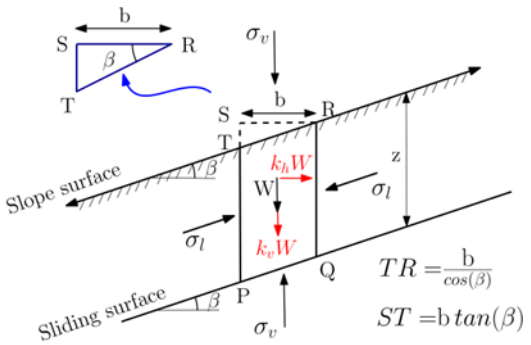

Figure 1. Stress state of an infinite slope under cyclic loading.

Figure 1 schematically represents the stress conditions within an infinite sandy slope of inclination β subjected to cyclic

(seismic) loading. In this study, the cyclic loading is idealised as sinusoidal ground accelerations, parameterised by the horizontal (k_h) and vertical (k_v) seismic coefficients, which represent the respective fractions of gravitational acceleration applied as inertial forces during shaking events. Following the framework proposed by (Biondi et al., 2000), this study incorporates stress-induced anisotropy using an anisotropic stress ratio, k_c, to better represent the evolving in-situ stress state under cyclic loading. The soil mass is assumed to be dry and cohesionless. The analysis considers an idealised infinite slope geometry to simplify boundary effects and focus on internal stress redistribution.

A representative soil element at depth z below the slope surface is considered. The stress acting on the vertical face in the downslope direction is denoted by σ_l, while the stress acting on the face parallel to the slope is denoted by σ_v, as shown in Figure 1. Under at-rest conditions, the relationship between these stresses can be defined using the lateral earth pressure coefficient.

To evaluate the principal stress state, these in-slope stresses are resolved into normal and shear components along a potential failure plane. For infinite slopes, it is assumed that the failure plane inclination α is equal to the slope angle β. Figure 2 shows the normal and shear stress components acting on the soil element and their orientation. In the proposed analysis, k_h is considered negative to represent an upslope-directed acceleration acting opposite to the potential sliding mass, while k_v is taken as positive, indicating an upward-directed vertical acceleration.

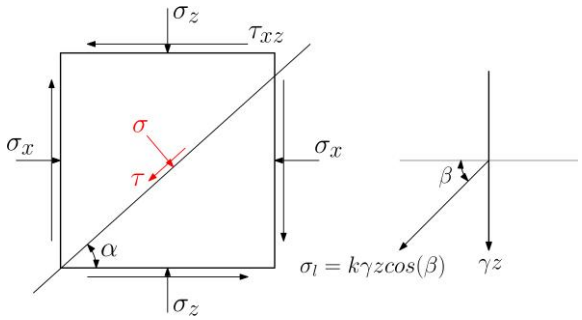

Figure 2. Stress components on the soil element and their orientation.

Therefore, the normal and shear stresses acting on the soil element are given by Equations (1), (2) and (3).

$$\sigma_x = -k_h \gamma z + k\gamma z cos^2\beta \quad (1)$$

$$\sigma_z = (1 - k_v)\gamma z + k\gamma z sin^2\beta \quad (2)$$

$$\tau_{xz} = k\gamma z\, cos\beta\, sin\beta \quad (3)$$

Now, the at-rest earth pressure condition for the slope is captured using the earth pressure coefficient at rest (k_0) given by Equation (4).

$$k_0 = \frac{\sigma_x}{\sigma_z} \quad (4)$$

By solving Equations (1), (2) and (4), the dimensionless coefficient k is obtained, as expressed in Equation (5). This parameter reflects the combined influence of the k_0, β, and the seismic coefficients (k_h and k_v)

$$k = \frac{k_0(1 - k_v) + k_h}{cos^2\beta - k_0\, sin^2\beta} \quad (5)$$

Now, principal stresses are derived from the normal and shear components using Mohr's circle relationships as indicated in Equation (6).

$$\sigma_{1,3} = \frac{\gamma z}{2}\left(A \pm \sqrt{B^2 + k^2 + 2Bkcos2\beta}\right) \quad (6)$$

Where A and B are dimensionless constants given by:

$$\text{A} = (1 - k_h - k_v + k) \text{ and B} = (-k_h + k_v - 1)$$

Also, the failure plane inclination can be expressed as shown in Equation (7).

$$\alpha = \frac{1}{2} tan^{-1}\left|\left(\frac{k\, sin\, 2\,\beta}{k\, cos\, 2\,\beta - 1 - k_h - k_v}\right)\right| \quad (7)$$

The principal stress ratio (k_c) at in-situ conditions, representing the stress anisotropy in the soil matrix can be obtained as shown in Equation (8).

$$k_c = \frac{\sigma_1}{\sigma_3} = \frac{A + \sqrt{B^2 + k^2 + 2Bkcos2\beta}}{A - \sqrt{B^2 + k^2 + 2Bkcos2\beta}}; \quad (8)$$

2.2 *Modified FOS for infinite sandy slopes considering stress-induced anisotropy*

The derived normal and shear stresses (Equations (1),(2) and (3)) are used to evaluate the stress state acting on any arbitrary failure plane inclined at angle α. Considering Figure 2, the stresses on this plane are given by Equations (9) and (10).

$$\sigma_n = \frac{\gamma z}{2}(A + (B + kcos2\beta)cos2\alpha + ksin2\beta sin2\alpha)) \quad (9)$$

$$\tau = \frac{\gamma z}{2}(-(B + kcos2\beta)sin2\alpha + ksin2\beta cos2\alpha)) \quad (10)$$

The FOS for failure along a plane inclined at angle α is given by the classical Mohr-Coulomb expression shown in Equation (11).

$$F = \frac{\sigma_n tan\emptyset'}{\tau} \quad (11)$$

Substituting the expressions for σ_n and τ (Equations (9) and (10)) and solving Equation (11) yields the modified FOS under cyclic loading, denoted by F_d (Equation (12)), which more accurately reflects the slope's resistance under seismic loading.

$$F_d = \frac{(A + (B + kcos2\beta)cos2\alpha + ksin2\beta sin2\alpha)) \times tan\emptyset'}{(-(B + kcos2\beta)sin2\alpha + ksin2\beta cos2\alpha)} \quad (12)$$

This analytical formulation introduces stress-induced anisotropy through the parameter k, which evolves based on the in-situ stress state under seismic excitation. Unlike traditional isotropic models, this framework allows the stress field to vary realistically during cyclic loading, thereby enhancing the accuracy of seismic slope stability prediction.

The proposed model calculates F_d for infinite sandy slopes subjected to cyclic seismic loads, incorporating key input variables such as β, k_h, k_v, k and soil strength properties reflected through the friction angle ϕ. The vertical stress is derived based on the slope inclination and overburden depth.

This formulation facilitates a streamlined yet mechanistically sound assessment of slope stability during seismic events, serving as the foundation for experimental comparison in the subsequent section.

3 EXPERIMENTAL COMPARISON

To assess the practical applicability and qualitatively validate the theoretical predictions of the proposed analytical model, a series of experimental studies was conducted using cyclic shear testing on sand samples. These experiments were designed to replicate key aspects of the analytical slope model, particularly the influence of slope angle, stress conditions, and cyclic loading on the development of stress-induced anisotropy.

Cyclic simple shear tests were performed using an EMDCSS apparatus (Figure 3) on dry, 100% sand specimens, representative of soils commonly encountered in the slope failures of the Western Ghats and Himalayan regions. The geotechnical properties of the sand determined experimentally through basic laboratory tests are listed in Table 1. Specimen preparation was carried out using the dry tamping method, ensuring uniformity and repeatability in density and structure. The specimens were compacted to a relative density of 30%. Cylindrical specimens of 20 mm height and 70 mm diameter were used for testing, consistent with apparatus dimensions and shear box configuration (Figure 3). The tests simulate different slope inclinations by varying the slope angle β to 20^0, 30^0, and 45^0, and applying corresponding stress states based on the analytical framework.

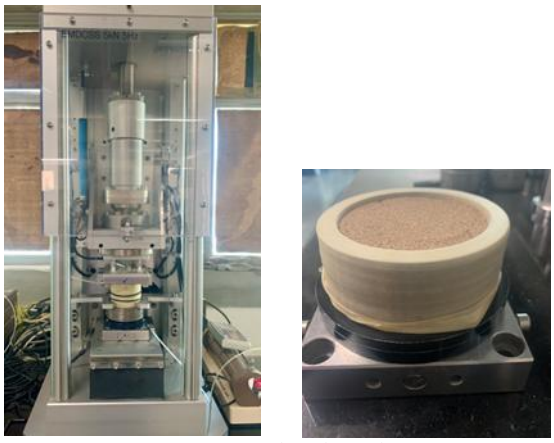

Figure 3. EMDCSS test set up and sand sample.

Each specimen was first subjected to the appropriate initial static stress condition, followed by cyclic loading with a horizontal seismic coefficient k_h= 0.15, representing moderate ground shaking. Simultaneously, the vertical acceleration effects, k_v, were considered as a fraction of k_h (0.5k_h). A loading frequency of 1 Hz was applied at 0.1mm amplitude for 100 loading cycles under dry conditions (Subhadarsini et al., 2020).

Table 1. Properties of sand (SP) used or the study.

Parameter	Symbol	Value	Unit
Specific gravity	G	2.63	-
Maximum Dry Density	γ_{dmax}	17.16	kN/m^3
Minimum Dry Density	γ_{dmin}	13.90	kN/m^3
Maximum void ratio	e_{max}	0.83	-
Minimum void ratio	e_{min}	0.48	-
Uniformity Coefficient	C_u	2.32	-
Coefficient of curvature	C_c	1.19	-

4 RESULTS AND DISCUSSIONS

4.1 *Analytical predictions of stress-induced anisotropy and slope stability*

Using the derived expression for the anisotropic stress ratio k_c, its variation with β was analysed under different levels of earthquake-induced loading, defined by the seismic coefficients k_h and k_v.

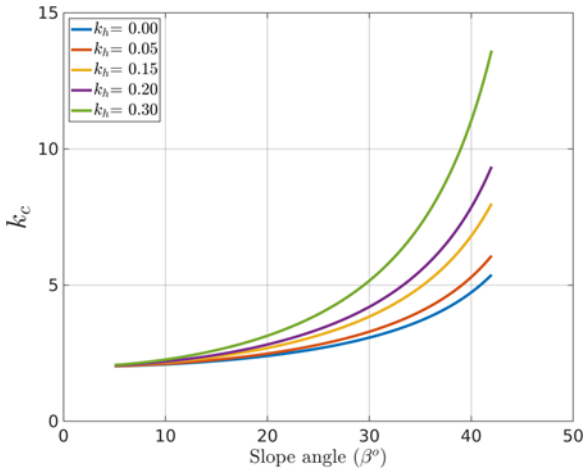

Figure 4. k_c variation with slope angle for different k_h.

As illustrated in Figure 4, k_c exhibits an increasing trend with both slope inclination and seismic intensity. This behaviour is attributed to the enhanced mobilisation of shear stress along the slope-aligned face as β increases. At higher slope angles, stress becomes increasingly unidirectional, intensifying stress anisotropy and resulting in a higher k_h. Similarly, an increase in seismic coefficients amplifies inertial forces, thereby disrupting stress equilibrium and contributing to an elevated anisotropic response.

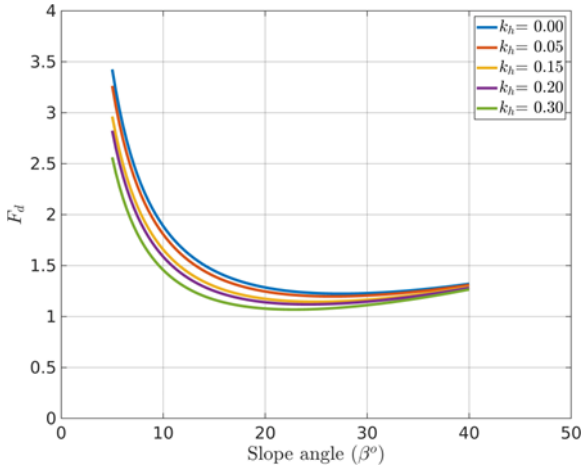

Figure 5. F_d variation with slope angle for different k_h.

Figure 5 presents the variation of the dynamic factor of safety F_d with slope angle. A general decrease in F_d with increasing β is observed, consistent with the destabilising influence of higher slope gradients. Notably, localised fluctuations in the trend, particularly between β=30^0 and 45^0 can be attributed to the non-linear nature of trigonometric terms within the dynamic equilibrium formulation. These oscillations occur due to the way seismic forces act along the slope direction and how stress-induced anisotropy varies with slope angle, which is a common complexity in dynamic soil behaviour for steep slopes. Experimental results for β=20^0, 30^0 and 45^0 yielded F_d values of 1.44, 1.41, and 1.39 respectively, showing a slight reduction with increasing β in line with the analytical trend. The small

discrepancy in absolute values is primarily due to the experimental loading being applied under k_0 conditions rather than the precise stress ratio assumed in the analytical model. Nevertheless, the agreement in trend between analytical and experimental results provides strong evidence for the reliability of the proposed framework in capturing the influence of stress-induced anisotropy on seismic slope stability.

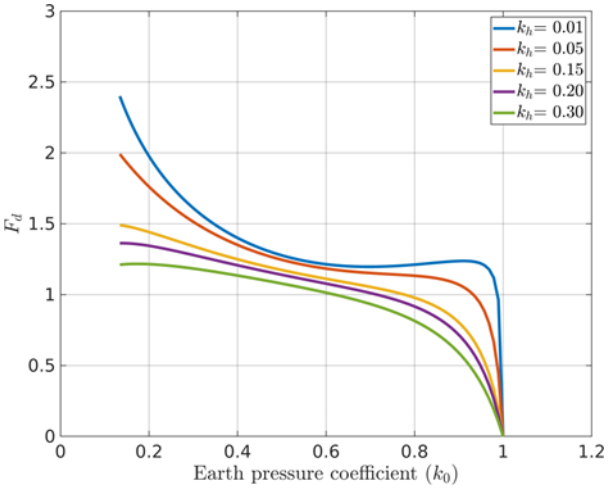

Figure 6. F_d variation with k_0 for different k_h.

Figure 6 illustrates the variation of F_d with k_0, for varying levels of seismic acceleration coefficient k_h. The results reveal a consistent trend of decreasing F_d with increasing k_0, indicating the crucial role of initial stress anisotropy in controlling slope stability under cyclic loading conditions. Physically, k_0 reflects the horizontal-to-vertical stress ratio and is directly influenced by the soil's internal friction angle ϕ through the empirical relation k_0=1−sinϕ (Jaky, 1948). A higher k_0 implies greater lateral confinement and less stress redistribution capability within the slope mass, which in turn reduces the mobilisation of shear resistance during dynamic excitation. Consequently, the slope becomes more susceptible to failure, resulting in a lower F_d. This effect is further intensified at higher seismic coefficients k_h, where the inertial forces magnify the impact of anisotropic stress conditions. These observations highlight the coupled influence of inherent soil strength parameters (like ϕ), initial stress anisotropy (via k_0), and dynamic loading (through k_h) on the seismic performance of slopes. Therefore, incorporating stress-induced anisotropy is essential for a realistic assessment of slope safety under earthquake loading.

4.2 *Experimental observations from cyclic simple shear testing*

The analytical findings were validated qualitatively using cyclic simple shear tests performed under k_0-conditions in the EMDCSS apparatus. The cyclic response for β= 20^0, 30^0 and 45^0 is presented in Figure 7, Figure 8 and Figure 9 respectively, through hysteresis loops obtained from the tests.

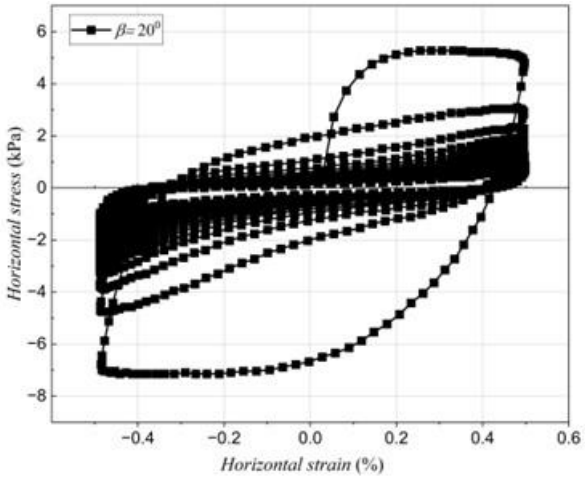

Figure 7. Stress-strain variations for β=20^0 slope condition.

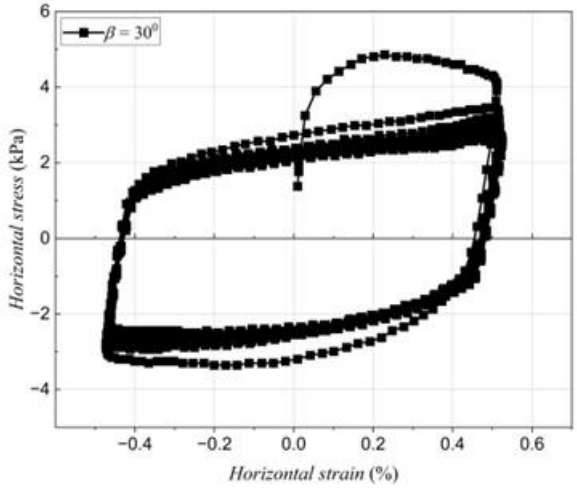

Figure 8. Stress-strain variations for β=30^0 slope condition.

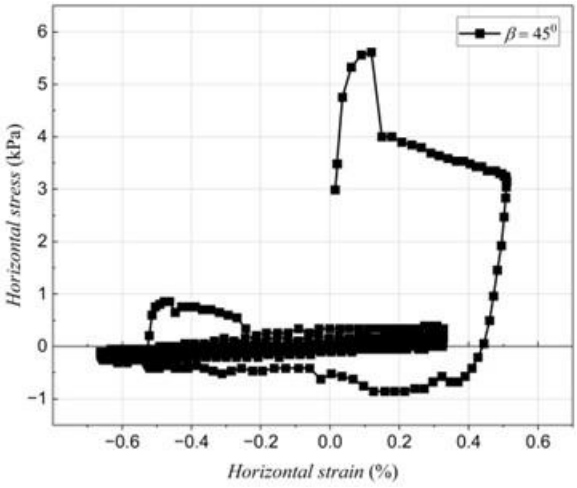

Figure 9. Stress-strain variations for β=45^0 slope condition.

The shape and area of hysteresis loops provide insight into soil behaviour. Energy dissipation, indicated by loop area, was highest for β=20^0 and reduced with increasing slope angle. This suggests greater damping and stiffness at lower inclinations. Specifically, the loop area reduced by approximately 33% between β=20^0 and 30^0, and by 66% between β=20^0 and 45^0, indicating enhanced damping capacity and stiffness at lower slope inclinations. Residual strain accumulation was minimal at β=20^0 and progressively increased with slope angle, indicating enhanced deformation potential and reduced cyclic

resistance at steeper slopes. The observed cyclic degradation trends support the analytical predictions, highlighting a qualitative correlation between increasing anisotropy and decreasing stability.

The CSR values extracted from the tests were 0.24, 0.27 and 0.42 for β= 20^0, 30^0 and 45^0. This increase in CSR with slope angle aligns with the analytical observation of decreasing F_d, suggesting a progressive rise in stress-induced anisotropy (i.e., higher k_c) leading to reduced stability. The inverse relationship between vertical stress and CSR further supports this trend, as steeper slopes reduce confinement and thus increase the mobilised cyclic stress relative to available resistance.

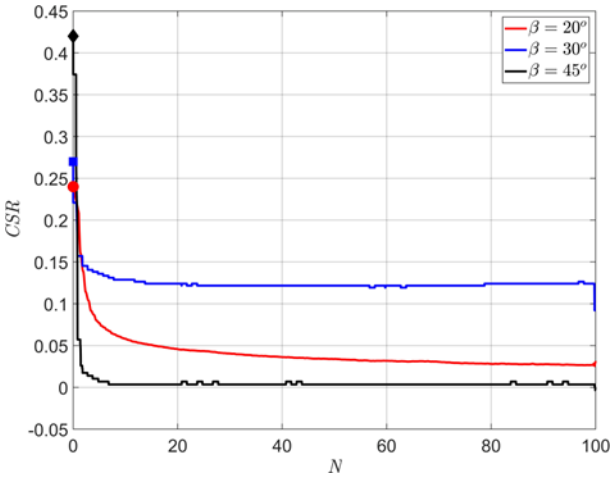

Figure 10. CSR variation with the number of cycles for different slope angles.

Figure 10 shows the smoothed CSR evolution with the number of cycles for the three slope angles. The rate of CSR reduction with loading cycles was highest for β= 45^0, indicating early onset of failure or deformation, whereas the slope with β= 20^0 demonstrated sustained resistance across more cycles. This further validates that steeper slopes not only mobilise higher cyclic stresses but also exhibit reduced endurance under repeated loading, consistent with the analytical trend of decreasing F_d.

4.3 *Correlation between CSR and k_c*

To further evaluate the compatibility between experimental observations and the analytical model, a linear regression analysis was performed between the CSR values from experimental data and k_c predicted from the analytical model for slope angles β=20^0, 30^0 and 45^0 (Figure 11). The corresponding k_c values were 2.69, 3.48 and 9.64, while the experimentally derived CSR values were 0.24, 0.27 and 0.42 respectively. The regression yielded Equation (13), with a high coefficient of determination R^2=0.997 and Pearson's correlation coefficient r =0.998, indicating an excellent linear relationship.

$$CSR = 0.177 + 0.025k_c \quad (13)$$

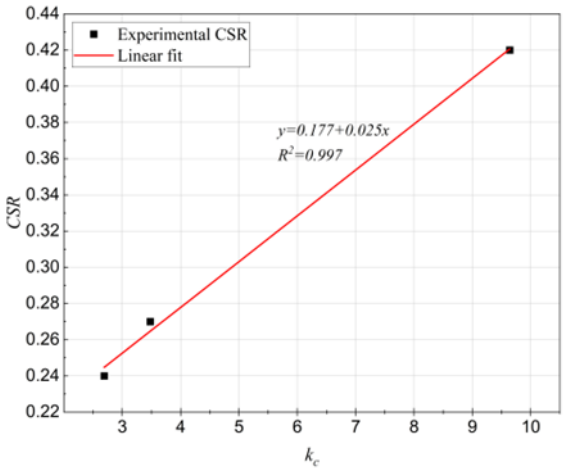

Figure 11. Correlation between CSR and k_c.

This strong correlation supports the inference that as β increases, k_c increases, leading to a higher CSR and consequently greater potential for residual deformation. The regression further validates the analytical model's ability to predict the influence of dynamic stress anisotropy on cyclic resistance.

5 SUMMARY AND CONCLUSIONS

An analytical framework was developed to evaluate the influence of stress-induced anisotropy on the stability of sandy slopes under cyclic loading. The model incorporates an anisotropic stress ratio as a function of β and seismic coefficients. The results showed that:

- k_c increases with both slope angle and seismic acceleration, indicating enhanced stress-induced anisotropy under steeper and more dynamically active conditions.
- F_d decreases with increasing β and seismic coefficients, reflecting reduced slope stability due to anisotropic stress redistribution. Analytical-experimental trends align despite magnitude differences due to k_0 vs. k_c conditions.
- The analytical results reveal a consistent reduction in F_d with increasing k_0, emphasising the critical role of stress-induced anisotropy in controlling seismic slope stability. This highlights the necessity of incorporating initial stress conditions in slope stability assessments.
- Experimental results from cyclic simple shear tests qualitatively validated the analytical trends.
- Energy dissipation (loop area) decreased significantly with increasing β by approximately 33% from β = 20^0 to 30^0, and by 66% from β = 20^0 to 45^0-suggesting greater damping and stiffness at lower inclinations.
- Residual strain accumulation increased with slope angle, indicating greater deformation potential and reduced cyclic resistance at steeper slopes.
- CSR also increased with slope angle, which aligns with the analytical observation of decreasing F_d and increasing k_c, reinforcing the conclusion that stress-induced anisotropy reduces slope stability under dynamic loading.
- A strong correlation between the analytical model and EMDCSS experimental results validates the reliability of the proposed anisotropic framework.

Overall, the experimental trends confirm the influence of stress-induced anisotropy on cyclic degradation and support the applicability of the developed analytical model in capturing the anisotropic behaviour of sandy slopes under seismic conditions.

6 LIMITATIONS AND FUTURE SCOPE

The analytical model developed captures the influence of stress-induced anisotropy under cyclic loading but has certain limitations. It does not account for liquefaction potential, pore pressure evolution, or inherent anisotropy, which are critical for a more complete understanding of seismic slope stability, especially in saturated soils.

While the derived expression generally shows a decreasing trend with increasing slope angle β, localised oscillations, particularly between $\beta = 30^0$ to 45^0, were observed. These arise from non-linear trigonometric interactions and variations in the seismic force projection and anisotropic response directionality, reflecting the complex behaviour of soil under steep, dynamic conditions.

The experimental validation remains qualitative, and future work should aim to quantitatively calibrate parameters like k_c using advanced tests such as cyclic triaxial or bender element tests. Extending the model to account for non-uniform soil profiles, depth-dependent loading, and multidirectional shaking would enhance its applicability to real-field scenarios.

7 ACKNOWLEDGEMENTS

The authors acknowledge the financial support received from the Indian Institute of Technology Hyderabad, Kandi, Sangareddy, Telangana, India, and the Ministry of Education (formerly known as the Ministry of Human Resource and Development), Government of India, which enabled the successful completion of this research.

8 REFERENCES

Asaoka, A., Noda, T., Yamada, E., Kaneda, K. and Nakano, M., 2002. An Elasto-plastic Description of Two Distinct Volume Change Mechanisms of Soils. *Soils and Foundations*, 42(5), pp.47–57. https://doi.org/10.3208/sandf.42.5_47.

Biondi, G., Cascone, E., Maugeri, M. and Motta, E., 2000. Seismic response of saturated cohesionless slopes. *Soil Dynamics and Earthquake Engineering*, 20(1), pp.209–215. https://doi.org/10.1016/S0267-7261(00)00051-8.

Chen, H., Wang, Y., Li, J. and Sun, D., 2020. A general failure criterion for soil considering three-dimensional anisotropy. *Computers and Geotechnics*, 125, p.103691. https://doi.org/10.1016/j.compgeo.2020.103691.

Fakharian, K., Kaviani-Hamedani, F. and Imam, S.M.R., 2022. Influences of initial anisotropy and principal stress rotation on the undrained monotonic behavior of a loose silica sand. *Canadian Geotechnical Journal*, 59(6), pp.847–862. https://doi.org/10.1139/cgj-2020-0791.

Gao, Y.-B., 2013. Compression and extension yield of an anisotropically consolidated soil. *Soils and Foundations*, 53(3), pp.431–442. https://doi.org/10.1016/j.sandf.2013.04.005.

Jaky, J., 1948. State of stress at great depth. In: *Proceedings of the Second International Conference on Soil Mechanics and Foundation Engineering, Rotterdam, Holland*. pp.103–107.

Manohar, R. and Saride, S., 2025. Influence of Stress-Induced Soil Anisotropy on Geotechnical Design: A Critical View. *Indian Geotechnical Journal*, pp.1–19. https://doi.org/10.1007/s40098-025-01239-x.

Shi W., Zhu J., He S. and Liu H., 2010. Stress-induced anisotropy of coarse-grained soil by true triaxial tests. *Chinese Journal of Geotechnical Engineering*, 32(5), pp.0–0.

Subhadarsini, S., Pradhan, S.P., Munda, J. and Pradhan, P.K., 2020. A PSO-Based Estimation of Dynamic Earth Pressure Coefficients of a Rigid Retaining Wall. In: A. Prashant, A. Sachan and C.S. Desai, eds. *Advances in Computer Methods and Geomechanics*. Singapore: Springer. pp.169–180. https://doi.org/10.1007/978-981-15-0890-5_15.

Zhang, F., Ye, B., Noda, T., Nakano, M. and Nakai, K., 2007. Explanation of Cyclic Mobility of Soils: Approach by Stress-Induced Anisotropy. *Soils and Foundations*, 47(4), pp.635–648. https://doi.org/10.3208/sandf.47.635.